

Supporting information for:  
Preferential protein depolymerization as a  
preservation mechanism for vascular litter  
decomposing in *Sphagnum* peat

1 Hendrik Reuter,<sup>\*,†</sup> Julia Gensel,<sup>†</sup> Marcus Elvert,<sup>‡</sup> and Dominik Zak<sup>¶</sup>

<sup>†</sup>*Department of Chemical Analytics and Biogeochemistry, Leibniz-Institute of Freshwater  
Ecology and Inland Fisheries, D-12587 Berlin, Germany*

<sup>‡</sup>*MARUM - Center for Marine Environmental Sciences and Faculty of Geosciences,  
University of Bremen, DE-28359 Bremen, Germany*

<sup>¶</sup>*Department of Bioscience, University of Aarhus, DK-8600 Silkeborg, Denmark*

E-mail: [hendrik.reuter@mail.de](mailto:hendrik.reuter@mail.de)

Table S1: Selected Data on Peatland Type, Pore Water and Peat Chemistry of the Sampling Sites.

	low-N substrate	medium-N substrate	high-N substrate
Name	Kablow-Ziegelei	Töpchin Süd	Stangenhagen
Coordinates	52°3273'N, 13°7274'E	52°1617'N, 13°5774'E	52°2081'N, 13°0941'E
Fen type	kettle hole mire	terrestrialisation mire	former percolation mire
Fen state	near pristine	near pristine	drained in 1967, agric. use, rewetted 1991, shallow lake
Peat type	<i>Sphagnum</i> spp.	sedge-brown-moss	~20 cm detritus mud over degraded peat
Dominant vegetation	<i>Sphagnum</i> spp., <i>Eriophorium angustifolium</i> <i>Vaccinium oxycoccos</i> <i>Drosera rotundifolia</i> <i>P. australis</i> (near ground water inputs)	<i>Carex</i> spp. brown mosses <i>P. australis</i> (in margin areas)	submerse vegetation <i>Typha latifolia</i> <i>P. australis</i> (in shallow areas, lake terrestrialisation)
<i>Pore water*</i>			
DOC (mg/L)	76.3 ± 17.1	19.6 ± 1.5	223 ± 43
pH	4.3 ± 0.5	6.6 ± 0.0	6.3 ± 0.1
electrical Conductivity (μS/cm)	60 ± 5	630 ± 24	2156 ± 308
SRP (mg/L)	0.02 ± 0.01	0.65 ± 0.27	10.82 ± 1.93
NO <sub>3</sub> <sup>-</sup> -N (mg/L)	<0.01	<0.01	<0.01
NH <sub>4</sub> <sup>+</sup> -N (mg/L)	1.0 ± 0.6	1.4 ± 0.7	71.6 ± 29.3
SO <sub>4</sub> <sup>2-</sup> (mg/L)	4.0 ± 0.9	11.5 ± 0.1	523 ± 176
Ca <sup>2+</sup> (mg/L)	4.3 ± 0.5	122 ± 6	173 ± 89
<i>Soil characteristics*</i>			
C (wt %)	43.3 ± 0.5	42.1 ± 0.1	28.1 ± 0.3
N (wt %)	1.31 ± 0.04	2.14 ± 0.02	2.29 ± 0.02
C/N (atom)	38.6	23.1	14.4
<i>Soil lignin*</i>			
P (mg/100mg C)	2.99	1.60	0.90
V (mg/100mg C)	0.99	2.29	1.30
S (mg/100mg C)	0.83	2.54	1.04
Ci (mg/100mg C)	0.96	2.30	0.64
Λ <sub>6</sub> (mg/100mg C)	1.83	4.83	2.34
P/V	3.01	0.70	0.69
S/V	0.84	1.11	0.80
Ci/V	0.96	1.00	0.49
(Ad/Al) <sub>V</sub>	0.50	0.33	0.83
(Ad/Al) <sub>S</sub>	0.50	0.41	0.73
CAD/FAD	1.23	1.04	0.85

SRP = Soluble Reactive Phosphorus, C = Carbon, N = Nitrogen, P = p-Hydroxy phenols, V = Vanillyl Phenols, S = Syringyl phenols, Ci = Cinnamyl Phenols, (Ad/Al)<sub>V</sub> = Ratio of vanillic acid to vanillin, (Ad/Al)<sub>S</sub> = Ratio of syringic acid to syringaldehyde, CAD/FAD = Ratio of p-coumaric acid to ferulic acid.  
\*data for the high-N substrate refer to the detritus mud.

Table S2: Parameters of the Peak Fitting Routine to fit Overlapping Bands in the FTIR Spectra of *P. australis* Litter using the Origin Peak Analyzer Tool.

Peak Position ( $\text{cm}^{-1}$ )	Gaussian Width ( $\text{cm}^{-1}$ )	Lorentzian Width ( $\text{cm}^{-1}$ )	Functional Group
1738	31.81	28.33	Aliphatic Ester Carbonyl Stretch
1720	60.78	0.02	Carboxylic Acid Carbonyl Stretch
1661	6.29E-5	82.87	Amide I
1632	43.62	81.19	Aromatic Skeletal Vibration
1604	21.97	4.85E-10	Aromatic Skeletal Vibration (8a)
1589	22.16	6.57	Aromatic Skeletal Vibration (8b)
1575	5.79E-7	78.89	Carboxylat
1541	0.12	62.93	Amide II
1513	18.49	11.56	Aromatic Skeletal Vibration (19a)
1463	3.33E-6	52.47	
1461	17.90	5.61	
1427	8.87	55.90	
1377	11.41	37.89	
1337	11.41	37.89	
1315	14.10	32.70	

A curve fitting was performed in the region 1850 to 1300  $\text{cm}^{-1}$  using OriginPro 8.5.0 Peak Analyzer software, Peak positions were determined from the second derivative spectra and peak widths were adjusted iteratively and from visual comparison with literature spectra of isolated biopolymers. Voigt-shape band widths were further optimized by difference spectroscopy of initial and decomposed leaf spectra. Special consideration was given to the carboxylate band at 1575  $\text{cm}^{-1}$  which strongly overlaps with amide II and increases during decomposition. Peak shape of this band was optimized from difference spectra of initial leaves and leaves that were subject to a short-time acid fumigation procedure with HCl (10 min). By acid fumigation, the carboxylate band disappears and the carboxylic acid band at 1720  $\text{cm}^{-1}$  increases. To achieve reproducible fits, constraints were imposed on Gaussian and Lorentzian peak widths and positions, leaving the peak height as only parameter to be optimized by the software. Before fitting, the baseline was set to zero at 1900  $\text{cm}^{-1}$  (what additionally required renormalization of spectra). Due to the increasing number of overlapping FTIR bands below 1500  $\text{cm}^{-1}$ , plotted bands below this wavenumber have only minor informative value but rather provide a baseline for peaks at higher wavenumber.

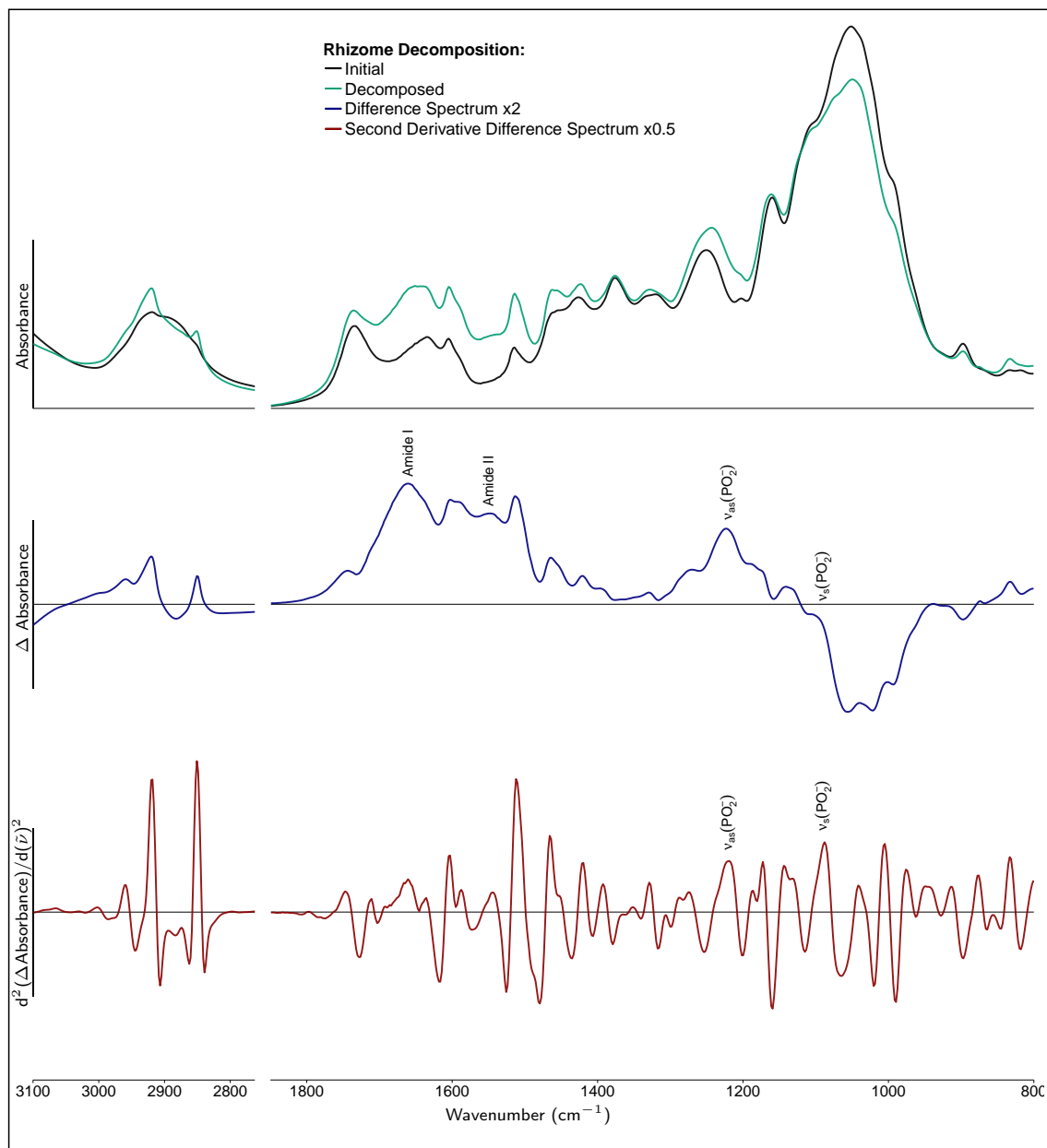


Figure S1: Exemplary figure on the formation of second derivative difference spectra using FTIR spectra of initial and decomposed rhizomes from the medium-N site. Shown above are the absorbance spectra, in the middle the difference spectrum (decomposed minus initial), and below the second derivative difference spectrum (multiplied with "-1") from which phosphodiester band increases are calculated. The size of the phosphodiester bands is derived from the peak height relative to the zero line.

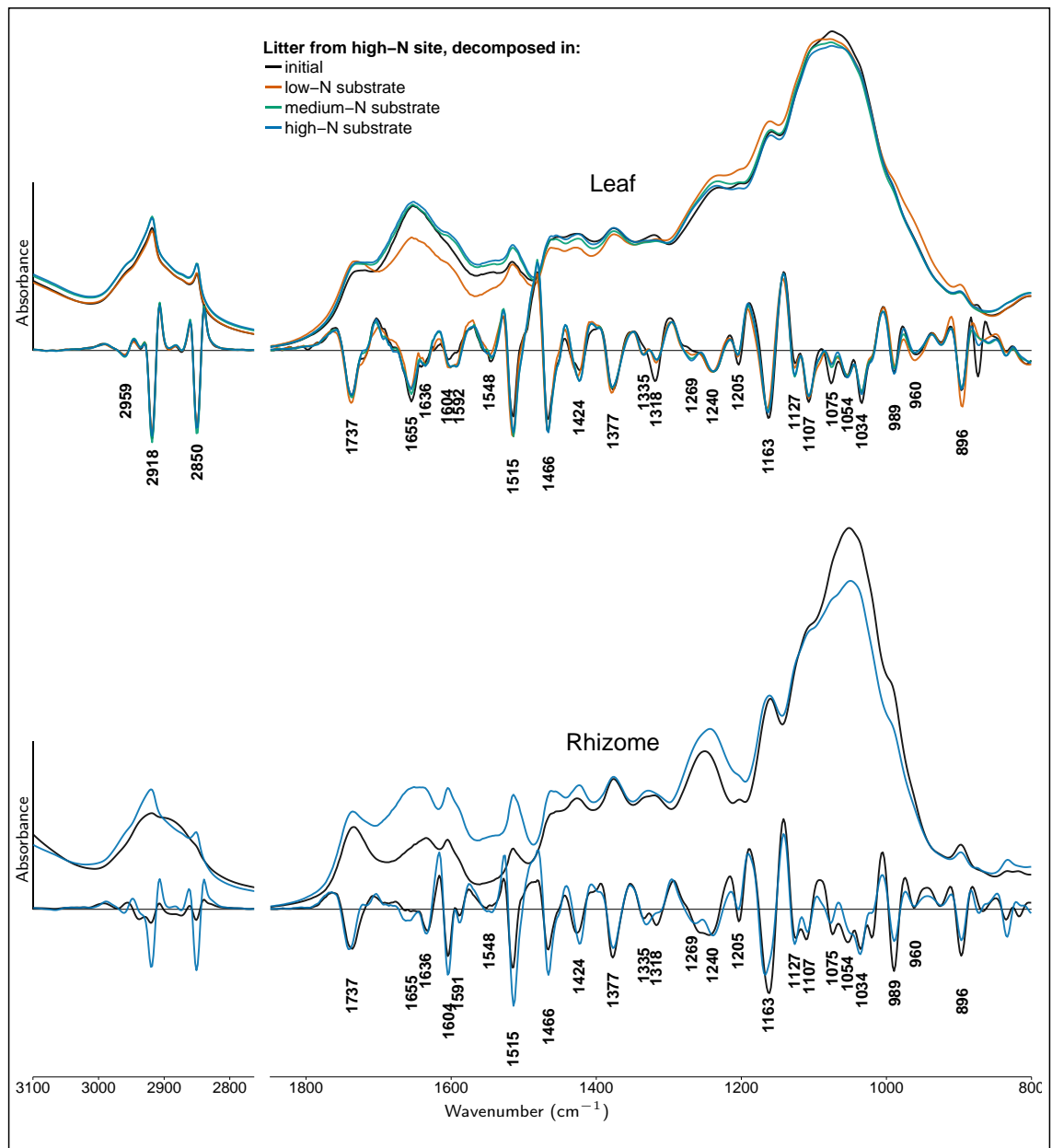


Figure S2: Absorption and second derivative infrared spectra of initial and decomposed leaves and rhizomes harvested from the rewetted fen Stangenhagen (high-N site). Leaves are the medium-N leaf litter. Leaves were decomposed in all three substrates, rhizome litter only in its home substrate. Shown are the mean of three replicate litter samples.

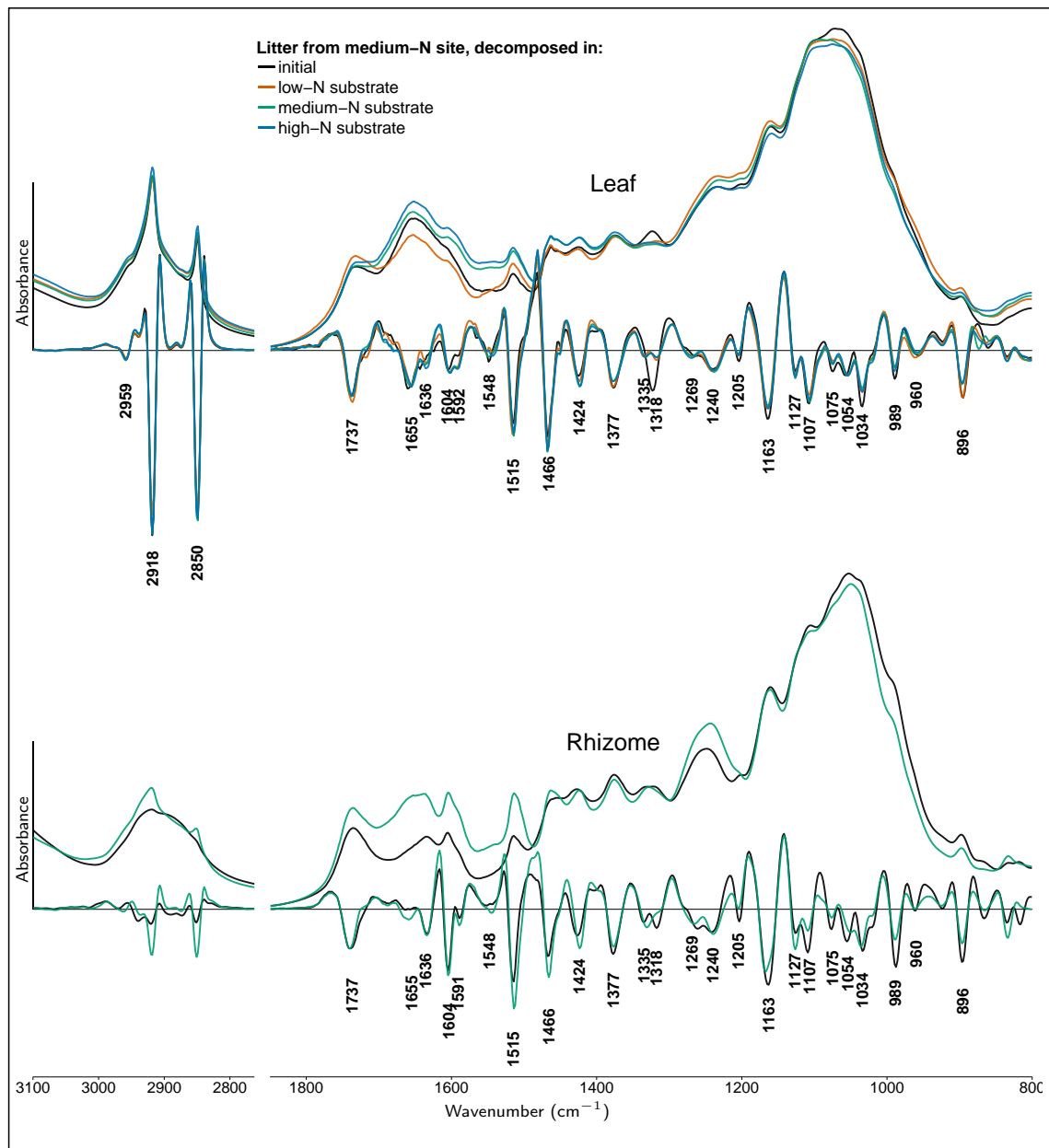


Figure S3: Absorption and second derivative infrared spectra of initial and decomposed leaves and rhizomes harvested from the brown-moss fen Töpchin Süd (medium-N site). Leaves are the low-N leaf litter. Leaves were decomposed in three substrates, rhizome litter only in its home substrate. Shown are the mean of three replicate litter samples.

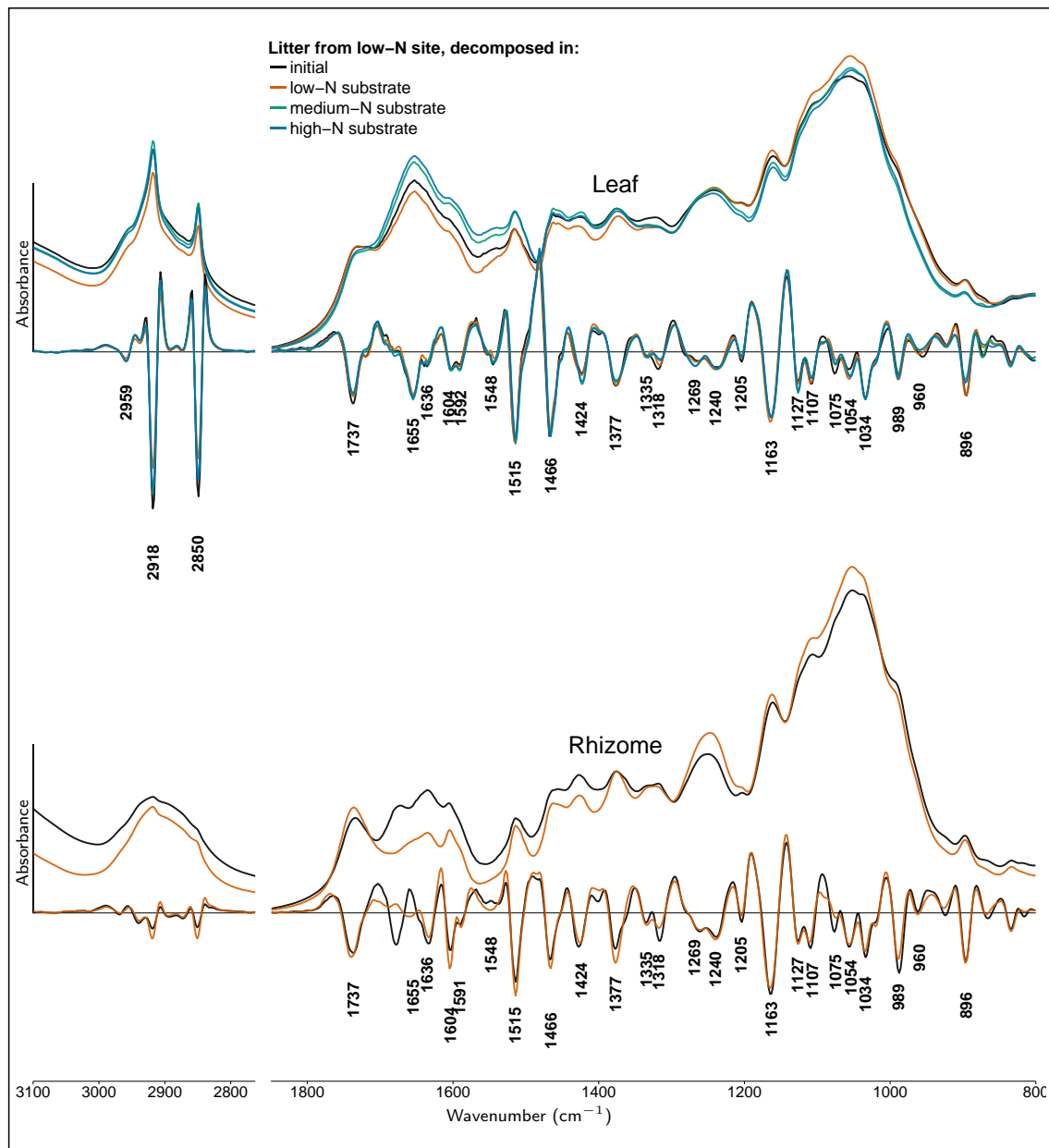


Figure S4: Absorption and second derivative infrared spectra of initial and decomposed leaves and rhizomes harvested from the *Sphagnum* peatland Kablow Ziegelei (low-N site). Leaves are the high-N leaf litter. Leaves were decomposed in three substrates, rhizome litter only in its home substrate. Shown are the mean of three replicate litter samples.

Table S3: Litter Raw Data with Sample Names for FTIR Spectra Assignment

Sample Name	Tissue	Origin	Decomposition Substrate	Mass Loss	C	N	Increase( $\nu_{as}(\text{PO}_2^-)$ )
				(%)	(wt%)	(wt%)	(a.u.)
LndK1	Leaf	low-N	initial	–	48.0	2.026	–
LndK2	Leaf	low-N	initial	–	45.7	2.28	–
LndK3	Leaf	low-N	initial	–	46.1	2.11	–
RndK1	Rhizome	low-N	initial	–	43.7	1.35	–
RndK2	Rhizome	low-N	initial	–	44.0	1.37	–
RndK3	Rhizome	low-N	initial	–	43.3	1.39	–
LndT1	Leaf	medium-N	initial	–	44.8	0.92	–
LndT2	Leaf	medium-N	initial	–	43.3	0.98	–
LndT3	Leaf	medium-N	initial	–	42.7	0.96	–
RndT1	Rhizome	medium-N	initial	–	42.9	0.14	–
RndT2	Rhizome	medium-N	initial	–	42.4	0.17	–
RndT3	Rhizome	medium-N	initial	–	41.8	0.14	–
LndS1	Leaf	high-N	initial	–	43.8	1.46	–
LndS2	Leaf	high-N	initial	–	41.5	1.39	–
LndS3	Leaf	high-N	initial	–	41.1	1.30	–
RndS1*	Rhizome	high-N	initial	–	42.7	0.32	–
RndS2	Rhizome	high-N	initial	–	41.6	0.29	–
RndS3	Rhizome	high-N	initial	–	42.8	0.26	–
1	Leaf	low-N	low-N	23.8	47.6	2.05	1.00
2	Leaf	low-N	low-N	26.4	47.8	2.26	1.24
3	Leaf	low-N	low-N	31.6	47.6	2.13	1.20
4	Leaf	low-N	medium-N	49.7	49.9	2.88	1.90
5	Leaf	low-N	medium-N	44.5	49.1	2.56	1.84
6	Leaf	low-N	medium-N	44.5	49.3	2.55	2.23
7	Leaf	low-N	high-N	43.7	48.6	2.95	1.91
8	Leaf	low-N	high-N	38.9	47.7	2.72	1.50
9	Leaf	low-N	high-N	43.8	48.3	2.83	1.85
10	Rhizome	low-N	low-N	34.6	45.7	0.29	1.15
11	Rhizome	low-N	low-N	38.1	45.7	0.31	0.88
12	Rhizome	low-N	low-N	37.1	45.9	0.30	0.51
13	Leaf	medium-N	low-N	33.7	43.2	1.26	1.51
14	Leaf	medium-N	low-N	33.2	43.4	1.16	1.41
15	Leaf	medium-N	low-N	29.5	43.5	1.10	1.49
16	Leaf	medium-N	medium-N	41.7	43.5	1.63	2.41
17	Leaf	medium-N	medium-N	45.7	43.7	1.74	2.14
18	Leaf	medium-N	medium-N	47.8	43.7	1.65	2.32
19	Leaf	medium-N	high-N	43.2	44.7	1.74	2.17
20	Leaf	medium-N	high-N	46.9	44.8	1.72	2.17
21	Leaf	medium-N	high-N	44.9	43.6	1.67	2.05
22	Rhizome	medium-N	medium-N	62.3	46.1	0.76	3.55
23	Rhizome	medium-N	medium-N	67.7	42.1	0.69	2.97
24	Rhizome	medium-N	medium-N	76.8	47.6	0.96	3.44
25	Leaf	high-N	low-N	20.7	41.4	1.17	0.76
26	Leaf	high-N	low-N	21.1	42.0	1.28	0.40
27	Leaf	high-N	low-N	20.9	42.7	1.14	0.37
28	Leaf	high-N	medium-N	40.1	42.9	1.82	1.30
29	Leaf	high-N	medium-N	39.1	42.9	1.88	1.29
30	Leaf	high-N	medium-N	41.0	43.5	1.83	1.27
31	Leaf	high-N	high-N	39.7	47.6	2.13	1.24
32	Leaf	high-N	high-N	37.0	43.9	1.81	1.06
33	Leaf	high-N	high-N	36.7	42.8	1.97	0.99
34	Rhizome	high-N	high-N	63.8	46.1	0.99	2.67
35	Rhizome	high-N	high-N	53.8	45.2	0.95	2.78
36	Rhizome	high-N	high-N	80.8	45.6	1.61	3.58

low-N = *Sphagnum* peat, medium-N = sedge-brown moss peat, high-N. = detritus mud. Raw data of FTIR spectra is available under <https://doi.pangaea.de/10.1594/PANGAEA.902069>. For each sample, an absorbance (x.abs) spectra and second derivative spectra (x.2der) is given. All spectra are vector normalized. In order to form the second derivative difference spectrum for a specific decomposed tissue according to Figure S5, the mean of three second derivative spectra of its undecomposed analogue must be subtracted from the samples second derivative spectra, the resulting spectra must be multiplied with "-1".

\* Spectrum not used.